

## STUDY OF TEMPERATURE DISTRIBUTION IN THE GROUND

Barbara Larwa\*, Krzysztof Kupiec

Cracow University of Technology, Faculty of Chemical Engineering and Technology,  
Warszawska St. 24, 31-155 Krakow

Knowledge of the temperature distribution in subsurface layers of the ground is important in the design, modelling and exploitation of ground heat exchangers. In this work a mathematical model of heat transfer in the ground is presented. The model is based on the solution of the equation of transient heat transfer in a semi-infinite medium. In the boundary condition on the surface of the ground radiation fluxes (short- and long-wave), convective heat flux and evaporative heat flux are taken into account. Based on the developed model, calculations were carried out to determine the impact of climatic conditions and the physical properties of the ground on the parameters of the Carslaw-Jeager equation. Example results of calculated yearly courses of the daily average temperature of the surface of the ground and the amount of particular heat fluxes on the ground surface are presented. The compatibility of ground temperature measurements at different depths with the results obtained from the Carslaw-Jeager equation is evaluated. It was found that the temperature distribution in the ground and its variability in time can be calculated with good accuracy.

**Keywords:** heat transfer, temperature distribution in the ground, heat balance at the ground surface

### 1. INTRODUCTION

Problems related to global warming and environmental pollution boost interest in alternative, renewable energy sources. Particularly noteworthy are systems with heat pumps, using the ground as the lower heat source. Heat pumps are environmentally friendly and energy-saving devices used for heating and cooling buildings, as well as heating domestic hot water. The ground can be used both as a heat source and as a heat sink. Heat transfer takes place when the ground is used in ground heat exchangers as a heat source/sink. To design a ground exchanger, knowledge of temperature distribution in the ground during different periods of the year is required. Experimental determination of temporal changes of temperature distribution in the ground is expensive, because measurement results should be averaged over many years; otherwise, the measured values will be random. Therefore, it is appropriate to develop a mathematical model for heat transfer in the ground and to formulate proper computational relationships.

The ground as a heat source, due to its high heat capacity, seems inexhaustible in this regard. However, the rate of heat transport is limited. If heat fluxes in the ground do not "keep up" with fluxes received by the ground heat exchanger, the ground cools down near the exchanger pipes, which significantly hampers its further operation. This condition is predictable through simulation calculations.

The ground can be treated as a system consisting of a subsurface layer, in which there are interactions related to changing weather conditions, and a deeper layer in which these impacts do not occur. The ground temperature, starting from a certain distance from the surface, is relatively stable. It is called the

\* Corresponding author, e-mail: bl@chemia.pk.edu.pl

undisturbed ground temperature, which depends on climatic conditions, and is different in various places of the Earth. Below the depth at which the impact of atmospheric conditions disappears, small changes in the ground temperature result from the existence of geothermal flux. However, its effect on the operation of horizontal ground heat exchangers is usually neglected.

The results of ground temperature measurements at various depths and in different places around the world are published in the literature. The results of extensive studies of temporal temperature changes of the ground at various depths under different climatic conditions in the USA have been presented by Kusuda and Achenbach (1965). Badache et al. (2016) showed the results of research carried out in Canada (Montreal), and Popiel and Wojtkowiak (2001; 2013) presented the results of research conducted in Poland (Poznan City).

Based on a theoretical analysis of thermal fluxes occurring on the surface of the ground, the temperature of the ground surface can be linked to the air temperature. Both of these quantities are time-dependent and defined by analytical relationships containing the cosine function. The parameters of these relationships are: annual average temperatures, annual fluctuation amplitudes and phase angles. These parameters are easily accessible for the air. In order to determine the parameters for the ground surface with known parameters for air, the heat balance on the ground surface should be considered and the dependence for determining individual heat fluxes should be formulated. Krarti et al. (1995) considered the following heat fluxes on the surface of the ground: solar radiation flux (short-wave), long-wave radiation flux, evaporative heat flux, convective heat flux, and conduction heat flux. Similar models were presented by other authors (Bortoloni et al., 2017; Freire et al., 2013; Fujii et al., 2012, 2013; Herb et al., 2008; Jaszczur et al., 2017; Mihalakakou et al., 1997; Nam et al., 2008; Ouzzane et al., 2014; Ouzzane et al., 2015; Staniec and Nowak, 2016). Most of these works assume that the long-wave radiation flux has a constant value equal to  $63 \text{ W/m}^2$ .

The most important parameter characterising the ground temperature is the average temperature of the surface of the ground which is equal to ground temperature at a great depth (undisturbed ground temperature). This quantity can be determined with good accuracy. One possibility is to use the empirical relationships presented by Gwadera et al. (2017). In these relationships, based on the heat balance on the ground surface, the dependence between the heat flux for moisture evaporation and the annual amount of precipitation was used.

This paper presents a model that takes into account the fact that long-wave radiation flux is subject to changes in the annual cycle. The solution to the model's equations allows determination of annual average temperature of the surface of the ground, the annual amplitude of temperature of the ground surface, and the phase angle of temperature. The impact of heat transfer coefficient between the surface of the ground and the air, amplitude of the air temperature and phase angle, as well as annual average solar radiation flux on the equation parameters were determined. Example results of calculations of daily average temperature of the ground surface and the amount of individual heat fluxes on the ground surface are presented. The calculations were carried out for moderate climate conditions. In addition, on the basis of data taken from the literature on ground temperature measurements at various depths, their compatibility with the Carslaw–Jaeger equation was evaluated.

## 2. CARSLAW–JAEGER EQUATION

For theoretical analysis of ground temperature changes with location and time the following assumptions are made:

- The ground is a homogeneous heat conducting medium,
- The ground can be treated as a semi-infinite medium with constant thermal diffusivity,

- The surface temperature of the ground is variable periodically over time,
- The geothermal gradient is zero.

The solution of the heat transfer equation under the above conditions was provided by Carslaw (1921) and Carslaw and Jaeger (1959). The daily average temperature of the ground  $T$  is the following function of position coordinate  $x$  and time  $t$ :

$$T = T_{sm} - A_s \cdot \exp\left(-\frac{x}{L}\right) \cdot \cos\left(\omega t - P_s - \frac{x}{L}\right) \quad (1)$$

The parameters of the above relationship are:  $T_{sm}$ ,  $A_s$ ,  $P_s$  and  $L$ . Damping depth  $L$  is defined as follows:

$$L = \sqrt{\frac{2a}{\omega}} \quad (2)$$

For phenomena occurring in the annual cycle, the frequency is equal to  $\omega = 2\pi/365 \text{ days}^{-1} = 0.199 \times 10^{-6} \text{ s}^{-1}$ .

The average value of the geothermal gradient on Earth is approx. 0.03 K/m, whereas the average value of the thermal conductivity of the ground is of the order of 1.5 W/(mK). Thus, the average geothermal heat flux density is  $0.03 \times 1.5 = 0.045 \text{ W/m}^2$ . It is a much smaller value than the other heat fluxes on the surface of the ground, which means geothermal flux can be neglected in balancing heat fluxes.

Due to neglecting the geothermal flux, the value of the annual average temperature of the ground practically does not depend on the position, i.e. the undisturbed ground temperature and the average temperature of the ground surface are the same.

The phase angle  $P$  is related to time elapsed from the beginning of the calendar year until the daily average value (temperature or flux) reaches the minimum, as follows:

$$P = \omega t_{\min} \quad (3)$$

Example profiles of the ground temperature are presented in Figs. 1a, b. Profiles of the ground temperature for different values of  $T_{sm}$  and  $A_s$  are shown in Fig. 1a while the impact of  $P_s$  and  $L$  on the ground temperature profiles is illustrated in Fig. 1b. Profiles apply to the 106<sup>th</sup> day of the calendar year. As can be seen from Fig. 1a, the average temperature of the ground surface has a strong effect on the temperature profile in the ground. However, the shape of the profile does not change for the same value of amplitude  $A_s$ . In turn, for a constant value of  $T_{sm}$  an increase in the amplitude  $A_s$  results in changes of temperature of the

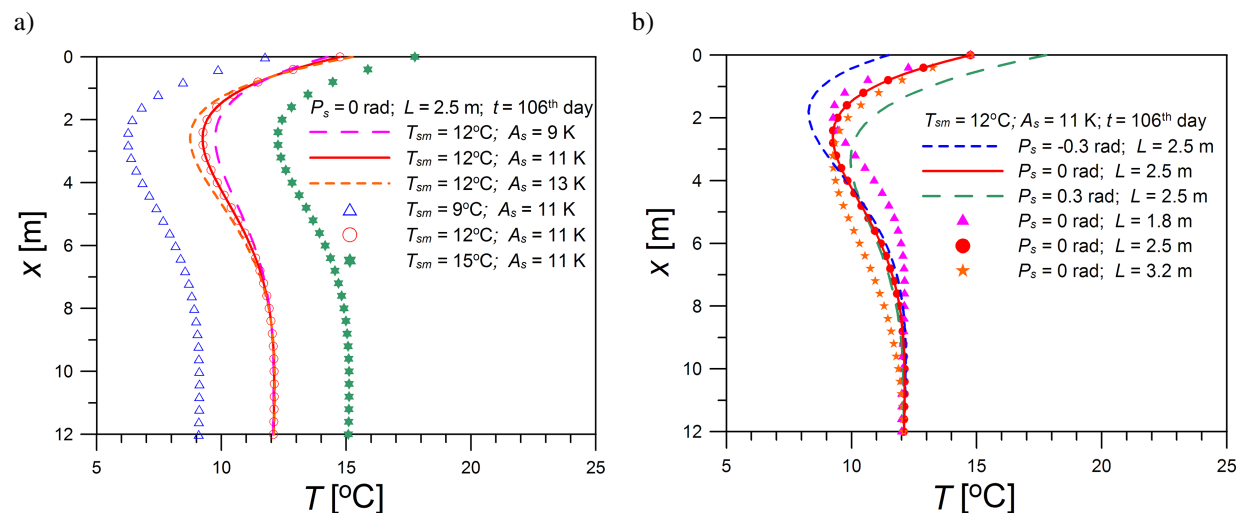


Fig. 1. Temperature profiles in the ground for different values of: a)  $T_{sm}$  and  $A_s$ , b)  $P_s$  and  $L$

ground, but only close to the place where the ground temperature is extreme. The damping depth  $L$  strongly affects the shape of temperature profile. With the higher  $L$  value, the depth at which the ground temperature remains unchanged with the position is larger. For example, at  $L = 1.8$  m the ground temperature reaches  $12\text{ }^{\circ}\text{C}$  ( $= T_{sm}$ ) starting from  $x \approx 6.5$  m, whereas at  $L = 3.2$  m the ground temperature stabilisation occurs for  $x > 12$  m. Furthermore, the phase angle  $P_s$  results in a strong change in the ground temperature only at small depths (up to a depth of approx. 4 m).

### 3. MATHEMATICAL MODEL OF HEAT TRANSFER IN THE GROUND

In numerical calculations the ground is treated as a plate with a finite thickness. Heat transfer in the ground under natural conditions is a cyclic steady state process. On the upper surface of the plate (the ground surface) periodically variable heat fluxes occur. These fluxes are variable both in the annual and daily cycles. Daily damping depth is, according to Eq. (2), approx.  $\sqrt{365} \cong 19$  times smaller than the annual damping depth. It is generally accepted that the range of ground temperature changes resulting from annual cycles does not exceed several meters. Therefore, changes resulting from daily cycles occur at depths of less than 1 m. Hence, considering the depth of the ground as less than 1 m, daily average values of heat fluxes can be used.

Geothermal flux has, in general, a slight impact on the ground temperature profile and will not be taken into account in this work.

On the surface of the ground the following heat fluxes: conductive, convective and thermal radiation fluxes can be listed. Moreover, on the surface of the ground moisture evaporation accompanied by phase change heat transfer should be mentioned.

#### 3.1. Convective heat flux

Convective heat flux is determined by the heat transfer equation:

$$H = h(T_a - T_s) \quad (4)$$

The heat transfer coefficient  $h$  is difficult to determine and depends on many parameters. The simplest empirical formulas determine the dependence of the  $h$  coefficient on wind velocity as the quantity having a major impact on the intensity of the convective heat transfer.

Daily average air temperature changes in the annual cycle as follows:

$$T_a = T_{am} - A_a \cos(\omega t - P_a) \quad (5)$$

The daily average temperature of the surface of the ground is periodically variable, like the air temperature:

$$T_s = T_{sm} - A_s \cos(\omega t - P_s) \quad (6)$$

The parameters of Eq. (6)  $T_{sm}$  and  $A_s$  are different from the corresponding parameters  $T_{am}$  and  $A_a$  for the air; the values of phase angles  $P_a$  and  $P_s$  are also different.

#### 3.2. Radiation heat fluxes

There are two types of thermal radiation fluxes on the surface of the ground: short- and long-wave. The short-wave flux comes from solar radiation. For balance calculations it is convenient to use a daily average

solar radiation flux absorbed by the ground  $S$  (the incident radiation flux is greater than  $S$  due to the partial reflection of sunlight on the ground surface). The solar radiation flux  $S$  changes in the annual cycle as follows:

$$S = S_m - A_{sol} \cos(\omega t - P_{sol}) \quad (7)$$

Because the temperature of the ground surface  $T_s$  is higher than the sky temperature  $T_{sky}$ , the ground radiates heat energy. Due to the low temperature of the radiation source, this type of radiation is long-wave. The daily average net flux of long-wave radiation  $LW$  equals:

$$LW = \varepsilon\sigma (T_s^4 - T_{sky}^4) \quad (8)$$

The expression in brackets can be represented in the following linearised form, in which the arithmetic average  $T_{m,ar}$  and the geometric average  $T_{m,g}$  from  $T_s$  and  $T_{sky}$  temperatures occur:

$$T_s^4 - T_{sky}^4 = \left[ (T_s + T_{sky})^2 - 2T_s T_{sky} \right] (T_s + T_{sky}) (T_s - T_{sky}) = 4 (2T_{m,ar}^3 - T_{m,ar} T_{m,g}^2) (T_s - T_{sky}) \quad (9)$$

Due to small differences between  $T_s$  and  $T_{sky}$  temperatures, the following relationship is valid:  $T_{m,ar} \cong T_{m,g} \equiv T_m$ . Thus, the daily average long-wave radiation flux is:

$$LW \cong \varepsilon C_{LW} (T_s - T_{sky}) \quad (10)$$

where:

$$C_{LW} = 4\sigma T_m^3 \quad (11)$$

The sky temperature  $T_{sky}$  depends on air temperature and its humidity. Temporary variability of sky temperature is determined by the dependence:

$$T_{sky} = T_{sky,m} - A_{sky} \cos(\omega t - P_a) \quad (12)$$

The values of the phase angle of the temperature of air and sky are similar. Assuming the value of 278 K as the mean value of the annual average temperatures  $T_{sm}$  and  $T_{sky,m}$   $C_{LW} = 4.83 \text{ W}/(\text{m}^2 \cdot \text{K})$  is obtained.

### 3.3. Evaporative heat flux

The stream of moisture is caused by a difference in the partial pressures of water vapour on the surface of the ground and in the bulk of the gaseous phase. This mass flux is connected with the heat flux transfer that is required for the evaporation of water, the heat being lost by the ground. This heat flux amounts to:

$$EV = f k_p (p_i - p) L_{evap} \quad (13)$$

The evaporation rate coefficient  $f$  takes into account the condition that the rate of evaporation of water from the ground surface is lower than the rate of evaporation from the water surface. This factor ranges from 0.1 to 0.2 for dry soils and up to 0.4–0.5 for humid soils (Krarti et al., 1995). The Chilton–Colburn analogy of heat and mass transfer (Cengel and Ghajar, 2010) results in a dependence between heat and mass transfer coefficients, leading to the following relationship:

$$EV = C_{EV} f h (p_i - p) \quad (14)$$

where:

$$C_{EV} = \frac{L_{evap} M_w}{P_0 M_a c_a} \left( \frac{D}{a_a} \right)^{2/3} \quad (15)$$

The quantity  $C_{EV}$ , determined according to the formula (15) at 10 °C, is assumed to be a constant:  $C_{EV} = 0.0168 \text{ K}/\text{Pa}$  (Krarti et al., 1995).

The quantity  $p_i$  is the saturated vapour pressure at the temperature of the ground surface ( $= P_{sat,s}$ ), while  $p = RH \cdot P_{sat,a}$ . Assuming a linear form of the relationship of saturated vapour pressure and temperature:  $P_{sat} = a_p T + b_p$ , the following expression is obtained:

$$EV = C_{EV} f h (P_{sat,s} - RH \cdot P_{sat,a}) \cong C_{EV} f h [(a_p T_s + b_p) - RH \cdot (a_p T_a + b_p)] \quad (16)$$

The values of constants are:  $a_p = 103 \text{ Pa/K}$ ,  $b_p = 609 \text{ Pa}$  (Krarti et al., 1995).

### 3.4. Heat balance on the surface of the ground

The heat balance on the surface of the ground has the form (Fig. 2):

$$q_{cond} = H - LW + S - EV \quad (17)$$

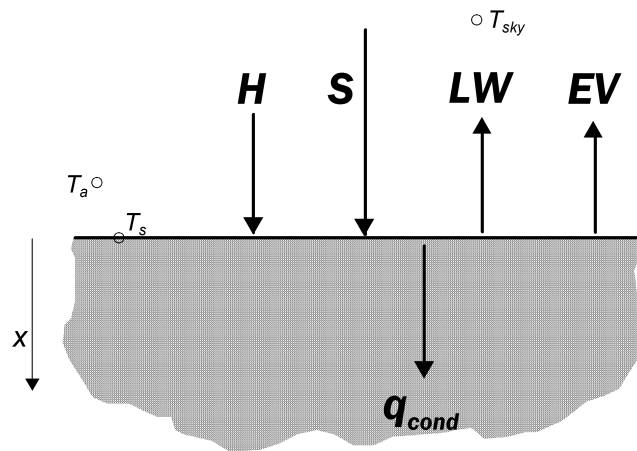


Fig. 2. Heat fluxes on the surface of the ground

The directions of the fluxes  $q_{cond}$  and  $H$  are variable with time. Convective heat flux is determined by Equation (4), whereas conductive heat flux is equal to:

$$q_{cond} = -k \left( \frac{\partial T}{\partial x} \right)_{x=0} \quad (18)$$

If  $T_a > T_s$ , then  $H > 0$  and the convective heat flux is directed from the air to the ground surface (Fig. 2). If  $(dT/dx)_{x=0} < 0$ , then  $q_{cond} > 0$  and the conductive heat flux is directed from the ground surface to its interior (Fig. 2). An equation analogous to Eq. (17) can be written in terms of the yearly average fluxes:

$$q_{cond,m} = H_m - (LW)_m + S_m - (EV)_m \quad (19)$$

Because the ground is in a cyclic steady state, the yearly average value of the conductive flux is zero:

$$q_{cond,m} = 0 \quad (20)$$

Yearly average values of other fluxes amount to:

$$H_m = h (T_{am} - T_{sm}) \quad (21)$$

$$(LW)_m = \varepsilon C_{LW} (T_{sm} - T_{sky,m}) \quad (22)$$

$$(EV)_m = C_{EV} f h [(a_p T_{sm} + b_p) - RH \cdot (a_p T_{am} + b_p)] \quad (23)$$

### 3.5. Calculation dependencies

Equations (19)–(23) result in the value of the average annual temperature of the ground surface:

$$T_{sm} = \frac{\varepsilon C_{LW} T_{sky,m} + h p_r T_{am} + S_m - C_{EV} f h b_p (1 - RH)}{h p_e + \varepsilon C_{LW}} \quad (24)$$

where:

$$p_e = 1 + C_{EV} f a_p \quad (25)$$

$$p_r = 1 + C_{EV} f a_p \cdot RH \quad (26)$$

In the *Appendix*, a derivation of the dependence to determine the amplitude of the temperature of the ground surface  $A_s$  and phase angle  $P_s$  is presented. In order to determine the  $P_s$  value, the following equation is valid:

$$P_s = \tan^{-1} \frac{p_1 + p_2 (1 + p_3)}{p_1 (1 + p_3) - p_2} \quad (27)$$

The amplitude  $A_s$  can be determined from the formula:

$$A_s = \frac{h p_e L}{k} \cdot \frac{p_1 \cos P_s + p_2 \sin P_s}{1 + p_3} \quad (28)$$

The constants  $p_1$ – $p_3$  are equal to:

$$p_1 = A_{as}^* \cos P_a + A_{sol}^* \cos P_{sol} \quad (29)$$

$$p_2 = A_{as}^* \sin P_a + A_{sol}^* \sin P_{sol} \quad (30)$$

$$p_3 = \frac{L}{k} (h p_e + \varepsilon C_{LW}) \quad (31)$$

where  $A_{as}^*$  and  $A_{sol}^*$  are expressed as:

$$A_{as}^* = A_a \frac{p_r}{p_e} + A_{sky} \frac{\varepsilon C_{LW}}{h p_e} \quad (32)$$

$$A_{sol}^* = \frac{A_{sol}}{h p_e} \quad (33)$$

## 4. VARIABILITY OF THE CARSLAW–JAEGER EQUATION PARAMETERS

Based on the presented model, calculations were carried out to determine the impact of climatic conditions and physical properties of the ground on the parameters of Eq. (1):  $T_{sm}$ ,  $A_s$  and  $P_s$ .

In Fig. 3 the effect of the heat transfer coefficient on the surface of the ground  $h$  and the annual average solar radiation flux absorbed by the ground  $S_m$  on the annual average temperature of the ground surface  $T_{sm}$  is shown. Both of these quantities strongly affect the  $T_{sm}$  value. With the increase of  $h$ , the annual average temperature of the ground surface decreases, while the higher the  $S_m$  values, the higher the  $T_{sm}$ .

For large values of  $h$  the  $T_{sm}$  values stabilise; wherein they can be both greater and smaller than  $T_{am}$ . For  $T_{sm} = T_{am}$  the annual convective heat flux is zero; according to the balance equation (19), this corresponds to the dependence:

$$(EV) = S_m - (LW)_m \quad (34)$$



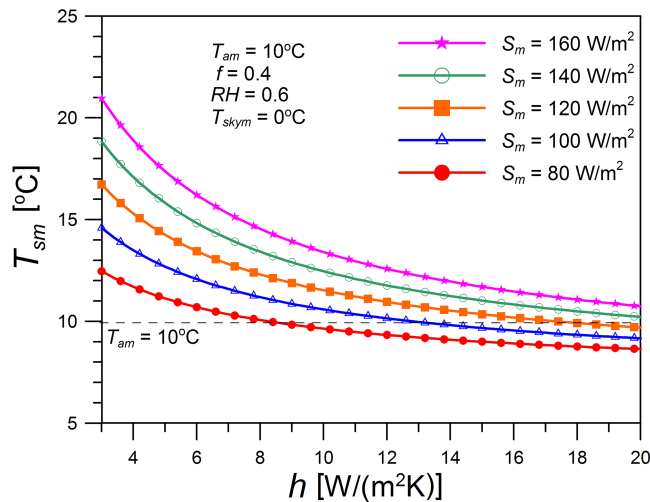


Fig. 3. Influence of  $h$  and  $S_m$  on  $T_{sm}$

In this particular case the yearly average evaporative heat flux equates to the yearly average net radiation flux.

Values of  $A_a$ ,  $A_{sol}$  and  $P_{sol}$  do not affect the annual average temperature of the surface of the ground  $T_{sm}$ .

Figure 4 pertains to the influence of various climatic conditions on the amplitude of ground surface temperature  $A_s$ . Particular attention was paid to the relationship between the quantities  $A_s$  and  $A_a$ . Small values of the air temperature amplitude and high relative humidity are characteristic of marine climate; these conditions correspond to a bunch of curves at the bottom of the chart. For small values of  $A_a$  there is the relation  $A_s > A_a$ . A bunch of curves at the top of the chart refer to climatic conditions in the hinterland; under these conditions the amplitudes of the air temperature are high, whereas the values of the relative humidity of the air are lower. For inland climate, variations in amplitudes of the temperature of the ground surface are smaller than the amplitudes of the air temperatures:  $A_s < A_a$ . The obtained regularities are consistent with measurement results presented by Kusuda and Achenbach (1965). Furthermore, it can be seen from Fig. 4 that the higher the  $h$  value and the lower the relative humidity,  $RH$ , the lower the  $A_s$  values.

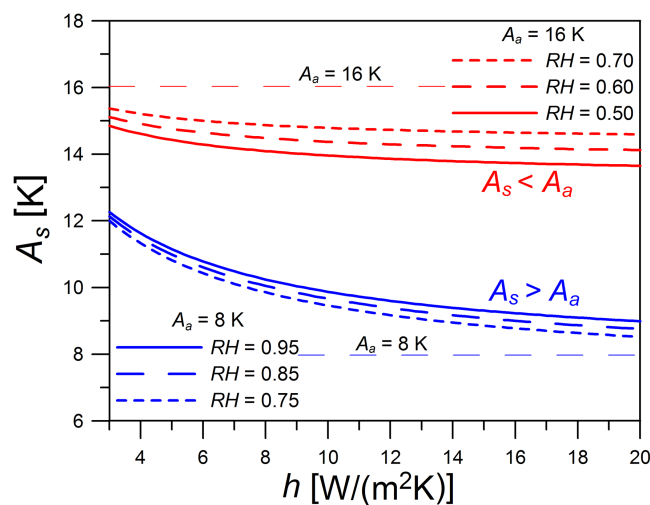


Fig. 4. Influence of  $h$  and  $A_a$  on  $A_s$

Values of  $T_{am}$ ,  $T_{sky,m}$  and  $S_m$  do not have any impact on the amplitude of the temperature of the ground surface  $A_s$ .



The impact of  $h$  and  $P_{sol}$  on the phase angle  $P_s$  is shown in Fig. 5. Values of  $P_s$  can both be positive and negative. Moreover, they can be both smaller and larger than  $P_a$  (Kusuda and Achenbach, 1965). For  $P_s < P_a$  the minimum temperature of the surface of the ground occurs earlier than the minimum air temperature. The heat transfer coefficient  $h$  as well as the phase angle of the solar radiation flux  $P_{sol}$  both exert a strong influence on  $P_s$ . Values of  $P_s$  increase with increasing  $P_{sol}$ , while the increase in  $h$  values of  $P_s$  progress towards  $P_a$ . In the extreme case of perfect convection ( $h \rightarrow \infty$ ) an equality:  $P_s = P_a$  takes place.

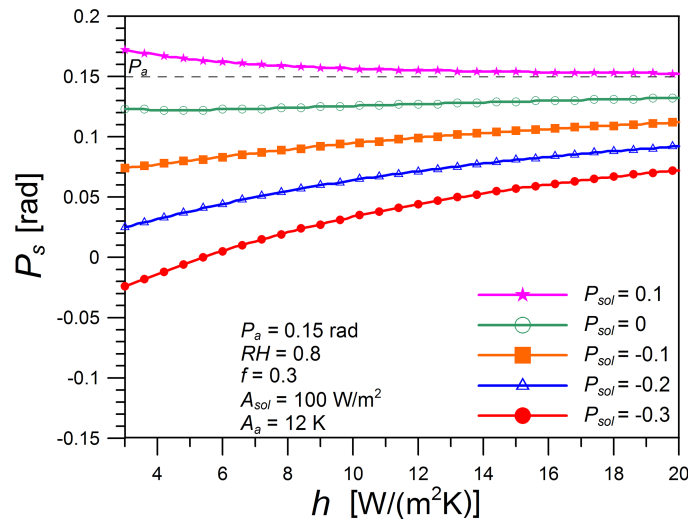


Fig. 5. Influence of  $h$  and  $P_{sol}$  on  $P_s$

Values of  $T_{am}$ ,  $T_{sky,m}$  and  $S_m$  do not have any impact on the phase angle of the temperature of the ground surface  $P_s$ .

Analysis shows that the heat transfer coefficient between the surface of the ground and air has a key impact on parameter values  $T_{sm}$ ,  $A_s$  and  $P_s$ .

## 5. DETERMINATION OF TEMPERATURE AND HEAT FLUXES ON THE SURFACE OF THE GROUND

Using the process model presented in Section 3, example calculations of temperature and heat fluxes on the ground surface were performed.

The values of the physical quantities used in the calculations are shown in Table 1.

Table 1. The numerical values used in the calculations

Quantity	Value	Quantity	Value
$T_{am}$	8.3 °C	$P_{sol}$	-0.153 rad
$A_a$	10.6 K	$RH$	0.79
$P_a$	0.270 rad	$k$	1.08 W/(m·K)
$T_{sky,m}$	-0.3 °C	$a$	$0.6 \times 10^{-6}$ m <sup>2</sup> /s
$A_{sky}$	11.6 K	$h$	13 W/(m <sup>2</sup> ·K)
$S_m$	119 W/m <sup>2</sup>	$\varepsilon$	0.9
$A_{sol}$	101 W/m <sup>2</sup>	$f$	0.3

Values regarding weather conditions correspond to the results of observations for Krakow-Balice (Poland), (Ministry of Investment and Development), developed in the form of approximation relations (Kicińska, 2018). It applies to the equation coefficients (5), (7) and (12). Temporal changes of relative humidity are irregular and difficult to describe; it was assumed that  $RH = \text{const}$ . Values of the heat transfer coefficient  $h$ , evaporation rate coefficient  $f$ , emissivity of the ground surface  $\varepsilon$ , thermal diffusivity of the ground  $a$ , and heat conduction coefficient  $k$  were assumed to be indicative. The time scale in Fig. 6 and Fig. 7 covers the whole calendar year.

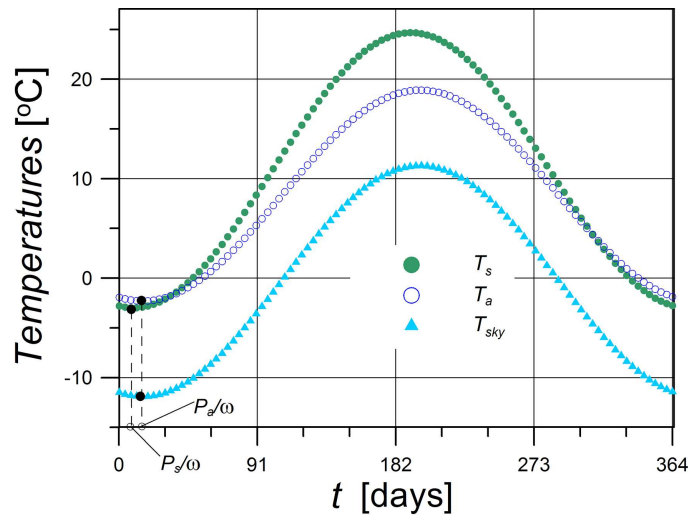


Fig. 6. Temporal courses of average daily ambient temperature, ground surface temperature and sky temperature

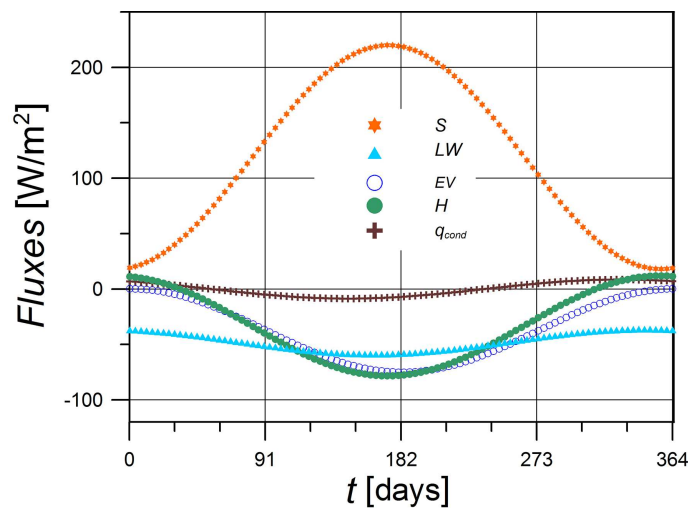


Fig. 7. Temporal courses of heat fluxes on the surface of the ground

In Fig. 6 annual courses of the average daily temperature of: the air  $T_a$ , the surface of the ground  $T_s$  and the sky  $T_{sky}$  are presented. The courses of temperatures  $T_a$  and  $T_{sky}$  correspond respectively to Equations (5) and (12), which are substituted with parameters listed in Table 1. The course of the temperature of the ground surface corresponds to Eq. (6) and values of parameters:  $T_{sm} = 10.9 \text{ }^\circ\text{C}$ ,  $A_s = 13.8 \text{ K}$ ,  $P_s = 0.166 \text{ rad}$  have been determined on the basis of the presented model. The courses of  $T_a$  and  $T_s$  are clearly different from each other. For a long period the temperature of the ground surface is higher than the air temperature. In the summer this difference is quite large.

The maximum daily average temperature of the surface of the ground ( $T_{sm} + A_s = 10.9 + 13.8 = 24.7$  °C) is higher than the maximum daily average temperature of the air ( $T_{am} + A_a = 8.3 + 10.6 = 18.9$  °C). Only in the short period during winter is the ground surface temperature lower than that of air. However, this difference is small.

The phase angles of the temperature of the surface of the ground and air can be assessed by the position of the points corresponding to the minimum temperatures. The minimum (as well as the maximum) value of  $T_s$  occurs earlier than the minimum (maximum) for  $T_a$ . The difference in phase angles  $\Delta P = P_s - P_a = 0.166 - 0.270$  corresponds to  $\Delta t = \Delta P / \omega \approx -6$  days. A similar result was observed by Popiel and Wojtkowiak (2013) a few days ahead of reaching the maximum value of  $T_s$  in relation to the maximum value of  $T_a$ .

The sky temperature  $T_{sky}$  is compatible in phase with the air temperature  $T_a$ . The value of  $T_{sky}$  is always lower than both the air temperature and the surface temperature of the ground.

The courses of heat fluxes on the surface of the ground are presented in Fig. 7. The course of solar radiation flux results from Eq. (7). The value of the long-wave radiation flux oscillates around a value of approximately  $50 \text{ W/m}^2$ . The heat flux due to evaporation of moisture from the ground changes significantly throughout the year; the highest value shows in the summer months, which is associated with a large difference in the temperatures of the ground surface and the air, generating the driving force of mass transfer in the form of the difference of partial pressures of water vapour on the surface of the ground and in the air. The directions of all three fluxes discussed so far are immutable: solar radiation flux is always directed towards the ground, and long-wave flux and evaporative heat flux are lost through the ground.

The convective heat flux changes its direction, which results directly from the relationship between  $T_s$  and  $T_a$ . However, since most of the year  $T_s > T_a$ , convective flux is responsible for the loss of heat from the ground. From the algebraic summation of all thermal fluxes on the surface of the ground results a stream transported to (or from) the interior of the ground  $q_{cond}$ . In spring and summer the conductive heat flux is directed from the surface to the inside of the ground, while in autumn and winter, heat from the deeper layers of the ground is transported towards the surface.

## 6. EXPERIMENTAL VERIFICATION OF CARSLAW–JAEGER’S EQUATION

Mathematical modelling is intentional as long as a model can be compared to reality. Often, full model verification is impossible. Because the presented model is based on the Carslaw–Jaeger Eq. (1), the latter was verified. For this purpose, measurement results presented by Popiel and Wojtkowiak (2013) were used. The measurements were carried out under moderate climate conditions (Poland). The temperature of the ground to a depth of 5 m between 1 pm and 3 pm was measured. Since the measurements were related to instantaneous temperatures (not to daily average), only results regarding the depth of the ground below 1 m were used for verification. Furthermore, only data regarding ground not covered with concrete were adopted. Measurements carried out at different times of the year: Jan 10<sup>th</sup>, Apr 3<sup>rd</sup>, Jul 3<sup>rd</sup> and Oct 4<sup>th</sup> were utilised. Nonlinear regression using the Solver application (Excel) was used to process results.

The sum of squares of differences between experimental and calculated temperatures according to Eq. (1) was minimised.

$$SS = \sum_{i=1}^n (T_{calculated} - T_{experimental})^2 \quad (35)$$

where  $n$  is the number of measurements used to develop results ( $n = 34$ ). The following values of parameters of Eq. (1) have been obtained:  $T_{sm} = 10.8$  °C,  $A_s = 10.4$  K,  $P_s = 0.393$  rad,  $L = 2.38$  m. In Fig. 8 the

comparison of experimental values and values calculated from Eq. (1) for the values of the parameters presented above is shown. Good compliance of the experimental and computational values confirms that Eq. (1) correctly describes the temperature distribution in the ground and its variability over time.

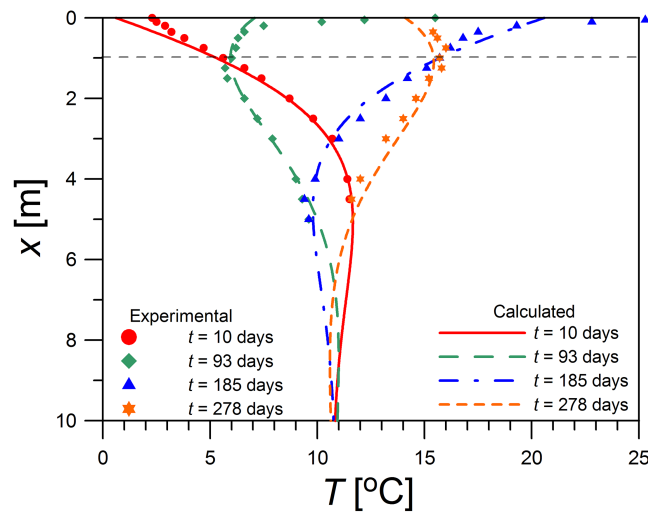


Fig. 8. Temperature profiles in the ground – comparison of experimental and computational results

Therefore, the temperature distribution in the ground and its temporal variability can be determined from the Carslaw–Jaeger equation, previously determining the parameters of this equation:  $T_{sm}$ ,  $A_s$ ,  $P_s$  and  $L$ . The following steps needed to be done:

- Determine the values that describe the daily average courses of the air and sky temperature, the solar radiation flux, and the relative humidity of the air.
- Determine the heat conduction coefficient and thermal diffusivity of the ground.
- Estimate the values of evaporation rate coefficient  $f$ , emissivity of the surface of the ground  $\varepsilon$ , and the heat transfer coefficient between the ground surface and the air  $h$ .
- Determine the parameters of the Carslaw–Jaeger Eq. (1) according to Eqs. (24), (27) and (28).

## 7. CONCLUSION AND FINAL REMARKS

- The Carslaw–Jaeger equation describes changes in ground temperature with depth and time correctly. Extensive measurements carried out by Kusuda and Achenbach (1965) show good compatibility with the equation. This consistency is also confirmed by results presented by Popiel and Wojtkowiak (2013); in this work, on the basis of these results, the parameters of the Carslaw–Jaeger equation were determined using the non-linear regression method.
- Based on the developed model, the impact of climatic conditions and physical properties of the ground on the parameters of the Carslaw–Jaeger equation was determined. The obtained calculation results in the form of relations between parameters for the ground and for the air are consistent with measurement results provided by Kusuda and Achenbach (1965).
- The presented mathematical model contains parameters that are difficult to determine:
  - Heat transfer coefficient  $h$ , depending on wind velocity,
  - Emissivity of the surface of the ground  $\varepsilon$ , depending on the type of coverage of the surface,
  - Evaporation rate coefficient  $f$ , depending on the humidity of the ground (this humidity is influenced by the amount of precipitation and ground permeability of water)

- Other factors that make determination of the temperature of the ground difficult are:
  - Variability of the thermal diffusivity of the ground with depth (the Carslaw–Jaeger equation, on which the presented model is based, applies to the constant thermal diffusivity of the ground),
  - The existence of snow cover in winter. The layer of snow with variable thickness and variable period of occurrence is an insulator that impedes heat transfer between the ground and the environment,
  - Freezing of the ground. Frozen ground has different thermal properties than unfrozen ground,
  - Convective heat transfer inside the ground due to groundwater movement.
- The ground temperature depends on many factors: latitude, weather conditions, season, altitude, terrain, shading, presence of buildings in the neighbourhood, type of surface coverage, land properties, and amount of precipitation. Since some of these quantities change irregularly, the ground temperature cannot be accurately predicted in any location or at any time, especially in places close to the surface of the ground.

### SYMBOLS

$a$	thermal diffusivity of the ground, $m^2/s$
$A$	amplitude of temperature, (K) or heat flux, ( $W/m^2$ )
$c_a$	specific heat of the air, $J/(kgK)$
$C_{EV}$	constant defined by Eq. (15), ( $= 0.0168 K/Pa$ )
$C_{LW}$	constant defined by Eq. (11), ( $= 4.83 W/(m^2K)$ )
$D$	diffusivity of water vapour in air, $m^2/s$
$EV$	evaporative heat flux, $W/m^2$
$f$	evaporation rate coefficient
$h$	convective heat transfer coefficient, $W/(m^2 \cdot K)$
$H$	convective heat flux, $W/m^2$
$k$	thermal conductivity of the ground, $W/(m \cdot K)$
$k_p$	mass transfer coefficient, $kg/(m^2 \cdot s \cdot Pa)$
$L$	damping depth, m
$L_{evap}$	latent heat of water evaporation, $J/kg$
$LW$	long-wave radiation heat flux, $W/m^2$
$M_a, M_w$	molar masses of the air and the water, $kg/kmol$
$p$	water vapour partial pressure, Pa
$P$	phase angle, rad
$p_e, p_r$	constants defined by Eqs. (25) and (26)
$P_{sat}$	water vapour saturation pressure, Pa
$P_0$	atmospheric pressure, Pa
$q$	heat flux, $W/m^2$
$q_{cond}$	conductive heat flux, $W/m^2$
$RH$	relative humidity of air
$S$	solar radiation flux absorbed by ground, $W/m^2$
$t$	time, s or days
$t_c$	cycle time, ( $= 365$ days)
$T$	ground temperature, $^{\circ}C$
$x$	position coordinate, m

#### Greek symbols

$\varepsilon$	emissivity of the ground surface
$\sigma$	Stefan-Boltzmann constant, ( $= 5.67 \cdot 10^{-8} W/(m^2 \cdot K^4)$ )
$\omega$	frequency, $s^{-1}$ or $days^{-1}$

*Subscripts*

<i>a</i>	ambient
<i>m</i>	yearly average value
<i>s</i>	the surface of the ground
<i>sol</i>	solar
<i>sky</i>	sky

## REFERENCES

- Badache M., Eslami-Nejad P., Ouzzane M., Aidoun Z., 2016. A new modelling approach for improved ground temperature profile determination. *Renewable Energy*, 85, 436–444. DOI: 10.1016/j.renene.2015.06.020.
- Bortoloni M., Bottarelli M., Su Y., 2017. A study on the effect of ground surface boundary conditions in modelling shallow ground heat exchangers. *Appl. Therm. Eng.*, 111, 1371–1377. DOI: 10.1016/j.applthermaleng.2016.05.063.
- Carslaw H.S., 1921. *Introduction to the mathematical theory of the conduction of heat in solids*. MacMillan and Co., Limited, London.
- Carslaw H.S., Jaeger J.C., 1959. *Conduction of heat in solids*. 2<sup>nd</sup> edition, Clarendon Press, Oxford.
- Cengel Y., Ghajar A., 2010. *Heat and mass transfer: Fundamentals and applications*. McGraw-Hill Education, New York.
- Freire A., Alexandre J.L.C., Silva V.B., Couto N.D., Rouboa A., 2013. Compact buried pipes system analysis for indoor air conditioning. *Appl. Therm. Eng.*, 51, 1124–1134. DOI: 10.1016/j.applthermaleng.2012.09.45.
- Fujii H., Nishi K., Komaniwa Y., Chou N., 2012. Numerical modelling of slinky-coil horizontal ground heat exchangers. *Geothermics*, 41, 55–62. DOI: 10.1016/j.geothermics.2011.09.002.
- Fujii H., Yamasaki S., Maehara T., Ishikami T., Chou N., 2013. Numerical simulation and sensitivity study of double-layer Slinky-coil horizontal ground heat exchangers. *Geothermics*, 47, 61–68. DOI: 10.1016/j.geothermics.2013.02.006.
- Gwadera M., Larwa B., Kupiec K., 2017. Undisturbed ground temperature – different methods of determination. *Sustainability*, 9, 2055. DOI: 10.3390/su9112055.
- Herb W.R., Janke B., Mohseni O., Stefan H.G., 2008. Ground surface temperature simulation for different land covers. *J. Hydrol.*, 356, 327–343. DOI: 10.1016/j.hydrol.2008.04.020.
- Ministry of Investment and Development, *TMY2 data*. Available at: <https://www.mir.gov.pl/media/51955/wmo125660iso.txt>. June 6<sup>th</sup> 2018.
- Jaszczur M., Polepszy I., Sapińska-Śliwa A., Gonet A., 2017. An analysis of the numerical model influence on the ground temperature profile determination. *J. Therm. Sci.*, 26, 82–88. DOI: 10.1007/s11630-017-0913-z.
- Kicińska I., 2018. *Analysis of heat fluxes on the surface of the ground*. Engineer's Thesis. Cracow University of Technology, Krakow.
- Krarti M., Lopez-Alonzo C., Claridge D.E., Kreider J.F., 1995. Analytical model to predict annual soil surface temperature variation. *J. Sol. Energy Eng.*, 117, 91–99. DOI: 10.1115/1.2870881.
- Kusuda T., Achenbach P.R., 1965. *Earth temperature and thermal diffusivity at selected stations in the United States*. National Bureau of Standards Report, Nr 8972, June 1965.
- Mihalakakou G., Santamouris M., Lewis J.O., Asimakopoulos D.N., 1997. On the application of the energy balance equation to predict ground temperature profiles. *Solar Energy*, 60, 3/4, 181–190. DOI: 10.1016/S0038-092X(97)00012-1.
- Nam Y., Ooka R., Hwang S., 2008. Development of a numerical model to predict heat exchange rates for a ground-source heat pump system. *Energy Build.*, 40, 2133–2140. DOI: 10.1016/j.enbuild.2008.06.004.
- Ouzzane M., Eslami-Nejad P., Badache M., Aidoun Z., 2015. New correlations for the prediction of the undisturbed ground temperature. *Geothermics*, 53, 379–384. DOI: 10.1016/j.geothermics.2014.08.001.

- Ouzzane M., Eslami-Nejad P., Aidoun Z., Lamarche L., 2014. Analysis of the convective heat exchange effect on the undisturbed ground temperature. *Solar Energy*, 108, 340–347. DOI: 10.1016/j.solener.2014.07.015.
- Popiel, C.O., Wojtkowiak J., Biernacka B., 2001. Measurements of temperature distribution in ground. *Exp. Therm Fluid Sci.*, 25, 301–309. DOI: 10.1016/S0894-1777(01)00078-4.
- Popiel C.O., Wojtkowiak J., 2013. Temperature distributions of ground in the urban region of Poznan City. *Exp. Therm Fluid Sci.*, 51, 135–148. DOI: 10.1016/j.expthermflusci.2013.07.009.
- Staniec M., Nowak H., 2016. The application of energy balance at the bare soil surface to predict annual soil temperature distribution. *Energy Build.*, 127, 56–65. DOI: 10.1016/j.enbuild.2016.05.047.

Received 26 June 2018

Received in revised form 16 January 2019

Accepted 15 February 2019

## APPENDIX

To the heat balance equation on the surface of the ground (17) dependencies on particular heat fluxes (18), (4), (10), (16) were substituted, considering the variability of temperatures over time (5), (6) and (12) and solar radiation flux (7). Following simplifications resulting from the balance of annual average heat fluxes (19)–(23) the following expression is obtained:

$$-k \left( \frac{\partial T}{\partial x} \right)_{x=0} = - \left( A_a h p_r + \varepsilon C_{LW} A_{sky} \right) \cdot \cos(\omega t - P_a) + A_s (h p_e + \varepsilon C_{LW}) \cdot \cos(\omega t - P_s) - A_{sol} \cdot \cos(\omega t - P_{sol}) \quad (A1)$$

The left side of (A1) can be represented in the form resulting from the differentiation of Eq. (1):

$$-k \left( \frac{\partial T}{\partial x} \right)_{x=0} = \frac{k}{L} A_s [\sin(\omega t - P_s) - \cos(\omega t - P_s)] \quad (A2)$$

Taking into account (A2) in Eq. (A1) the following formula is obtained:

$$A_s \left\{ -\frac{k}{L} [\sin(\omega t - P_s) - \cos(\omega t - P_s)] + (h p_e + \varepsilon C_{LW}) \cos(\omega t - P_s) \right\} = \left( h p_r A_a + \varepsilon C_{LW} A_{sky} \right) \cos(\omega t - P_a) + A_{sol} \cos(\omega t - P_{sol}) \quad (A3)$$

Substituting to Eq. (A3)  $t = 0$  the following expression is given:

$$A_s \left\{ \frac{k}{L} [\cos(-P_s) - \sin(-P_s)] + (h p_e + \varepsilon C_{LW}) \cdot \cos(-P_s) \right\} = \left( h p_r A_a + \varepsilon C_{LW} A_{sky} \right) \cdot \cos(-P_a) + A_{sol} \cos(-P_{sol}) \quad (A4)$$

However, after substituting  $t = P_s/\omega$  into Eq. (A3) this is attained:

$$A_s \left\{ \frac{k}{L} [\cos(0) - \sin(0)] + (h p_e + \varepsilon C_{LW}) \cos(0) \right\} = \left( h p_r A_a + \varepsilon C_{LW} A_{sky} \right) \cos(P_s - P_a) + A_{sol} \cos(P_s - P_{sol}) \quad (A5)$$

By dividing the above equations, Eq. (27) is obtained. After calculating the phase angle  $P_s$  amplitude  $A_s$  can be determined according to Eq. (28).